

## Clinical value of the *MGMT* promoter methylation score in IDHmt low-grade glioma for predicting benefit from temozolomide treatment

Amélie Darlix, Pierre Bady<sup>o</sup>, Jérémy Deverdun, Karine Lefort, Valérie Rigau<sup>o</sup>, Emmanuelle Le Bars, Justine Meriadec<sup>o</sup>, Mathilde Carrière, Arthur Coget, Thomas Santarius, Tomasz Matys<sup>o</sup>, Hugues Duffau<sup>o</sup> and , Monika E Hegi<sup>o</sup>

All author affiliations are listed at the end of the article

**Corresponding Author:** Monika E. Hegi, PhD, Centre Hospitalier Universitaire Vaudois, Lausanne University Hospital, Chemin des Boveresses 155, CLE-C 306, 1066 Epalinges, Switzerland ([monika.hegi@chuv.ch](mailto:monika.hegi@chuv.ch)).

### Abstract

**Background.** Diffuse IDH mutant low-grade gliomas (IDHmt LGG) (World Health Organization grade 2) typically affect young adults. The outcome is variable, with survival ranging from 5 to over 20 years. The timing and choice of initial treatments after surgery remain controversial. In particular, radiotherapy is associated with early and late cognitive toxicity. Over 90% of IDHmt LGG exhibit some degree of promoter methylation of the repair gene O(6)-methylguanine-DNA methyltransferase (*MGMTp*) that when expressed blunts the effect of alkylating agent chemotherapy, for example, temozolomide (TMZ). However, the clinical value of *MGMTp* methylation predicting benefit from TMZ in IDHmt LGG is unclear.

**Methods.** Patients treated in the EORTC-22033 phase III trial comparing TMZ versus radiotherapy served as training set to establish a cutoff based on the *MGMT*-STP27 methylation score. A validation cohort was established with patients treated in a single-center first-line with TMZ after surgery/surgeries.

**Results.** The *MGMT*-STP27 methylation score was associated with better progression-free survival (PFS) in the training cohort treated with TMZ, but not radiotherapy. In the validation cohort, an association with next treatment-free survival ( $P = .045$ ) after TMZ was observed, and a trend using RANO criteria ( $P = .07$ ). A cutoff value set above the 95% confidence interval of being methylated was significantly associated with PFS in the TMZ-treated training cohort, but not in the radiotherapy arm. However, this cutoff could not be confirmed in the test cohort.

**Conclusions.** While the *MGMTp* methylation score was associated with better outcomes in TMZ-treated IDHmt LGG, a cutoff could not be established to guide treatment decisions.

### Key Points

- Risk-adjusted treatment for patients with IDHmt low-grade glioma to preserve cognition and quality of life.
- *MGMTp* methylation score associated with better outcomes in temozolomide-treated patients.
- No robust *MGMTp* methylation cutoff for treatment decisions could be validated in the test cohort.

## Importance of the Study

Biomarkers for the identification of patients with IDHmt low-grade glioma, who may benefit from chemotherapy would enable safe de-escalation of treatment, by delaying radiotherapy. This would defer radiation-induced cognitive decline and preserve the quality of life in young patients with potentially long survival, while not compromising outcomes. In a previous study on a clinical trial cohort for high-risk low-grade glioma,

we found that the *MGMT* promoter methylation score was associated with good outcomes in temozolomide (TMZ)-treated patients that we confirmed in a real-world, single-institution cohort of patients treated with TMZ as first-line treatment after surgery constituted for this study. However, the cutoff established in the clinical trial cohort, intended to guide treatment decisions, could not be validated in the real-world patient cohort.

Diffuse IDHmt low-grade gliomas (IDHmt LGG) (World Health Organization [WHO] grade 2<sup>1</sup>) are rare tumors (yearly incidence 1 to 2/10<sup>5</sup>) typically affecting young patients in their third and fourth decades. These tumors are characterized by a mutation in the isocitrate dehydrogenase (*IDH*) gene 1 or 2 (IDHmt) that is associated with a CpG island methylator phenotype (CIMP). IDHmt LGG are slowly growing tumors that eventually progress, with a median overall survival (OS) of 5 to over 20 years.<sup>2–4</sup> The prognosis depends on the genetic subtype in particular the presence of a codeletion of the chromosomal arms 1p and 19q (further referred to as codeleted) as well as clinical and radiological parameters such as age, tumor size, and inherent growth rate. Maximal safe surgical resection is the first step in the management of the disease, as the extent of resection has a positive prognostic impact.<sup>5</sup> However, the timing and choice of further treatments, including chemotherapy, radiation therapy (RT), or combinations, remain controversial.<sup>6–9</sup> For more indolent IDHmt LGG, 1–5 years after their last resection, targeting the IDHmt enzymes with vorasidenib seems to improve progression-free survival (PFS) (hazard ratio [HR] 0.39).<sup>10,11</sup>

The EORTC-22033 randomized trial for high-risk LGG showed no difference in PFS between RT and temozolomide (TMZ) in the trial population, but variations were observed between the molecular subtypes.<sup>12</sup> In the subgroup analysis, patients with IDHmt non-codeleted tumors exerted longer PFS in the RT group, while no difference was observed for IDHmt codeleted patients treated with RT or TMZ. Yet, considering the risk of early and late neurocognitive toxicity<sup>13</sup> associated with RT, and in the absence of data on overall survival (OS), many physicians choose to delay RT. As the timing for RT was shown not to impact OS,<sup>14</sup> initial TMZ or the multidrug regimen with procarbazine, CCNU (Lomustine), and vincristine (PCV) has been considered as first-line medical treatment.<sup>15</sup>

In view of the potentially long survivorship of these patients, it is indeed crucial to propose risk-adapted treatment strategies, balancing efficacy and treatment-related short-/long-term toxicity affecting quality of life (QoL) and cognitive function. In this context, developing biomarkers to identify patients who benefit from TMZ is of utmost importance and will allow delaying RT and, consequently, avoiding or deferring RT-associated neurocognitive toxicity.

A prominent predictive marker for benefit from TMZ in patients diagnosed with glioblastoma is the

epigenetic silencing of the *O(6)-methylguanine-DNA methyltransferase (MGMT)* gene by promoter methylation. *MGMT* encodes a DNA repair protein that neutralizes the most cytotoxic lesion of alkylating agents (including TMZ) by removing the methylation at the O6-position of guanine. In glioblastoma patients, the *MGMT* promoter (*MGMTp*) methylation status is predictive of benefit from TMZ<sup>16</sup> and is now used to select patients into trials with or without alkylating agent therapy, respectively.<sup>17</sup> However, the impact of *MGMTp* methylation in IDHmt LGG patients receiving TMZ is not as clear. Most IDHmt LGG are classified as *MGMTp* methylated—almost 100% for codeleted and 90% for non-codeleted—hence highly associated with the CIMP.<sup>12,18</sup> In a translational research study, we used data from the EORTC-22033 randomized trial to investigate the role of *MGMTp* methylation in high-risk IDHmt LGG for predicting benefit from TMZ treatment.<sup>12</sup> In the TMZ-arm, a high *MGMTp* methylation score was predictive of a longer PFS, while no such effect was observed in the corresponding RT-arm.<sup>19</sup>

In this study, we aimed at validating a predictive impact of the *MGMTp* methylation score on PFS in an independent dataset of IDHmt LGG treated with TMZ only as first-line therapy after surgery. To this end, we used the EORTC-22033 patient population<sup>19</sup> as a training dataset to investigate the score and define new cutoff(s) and constituted an independent test dataset to validate the pertinence.

## Materials and Methods

### Patient Selection and Study Design

**Training cohort (EORTC-22033).**—The training cohort comprised patients enrolled in the phase III trial, EORTC-22033 randomizing high-risk LGG patients to TMZ or RT as previously described.<sup>12</sup> Patients with an IDHmt/CIMP LGG grade II (WHO 2016) for whom 450K DNA methylation data were available from the initial surgery, were included, and comprised 57 patients from the TMZ-arm and 63 from the RT-arm.<sup>19</sup> The comparison of the baseline characteristics of this cohort with the rest of the patients has been reported previously.<sup>19</sup> Patients in the TMZ-arm were treated with 75 mg/m<sup>2</sup> TMZ 21/28 days for 12 cycles or until progression. Clinical data, including criteria for treatment

initiation and definition of PFS, and molecular data have been reported previously.<sup>12,19</sup> The full methylome dataset is available under the accession number GSE104293 at GEO (<http://www.ncbi.nlm.nih.gov/geo/>).

### Patient Selection for the Test Cohort (Montpellier)

The test cohort was constituted retrospectively from a single center (Institut régional du Cancer Montpellier [ICM], France), including LGG patients treated with TMZ only, as first-line therapy after surgery/surgeries between 2002 and 2022. Patients were selected from the institutional “Neuro-oncology” database (BDD-NO) according to the following criteria: age  $\geq 18$ ; histologically confirmed supratentorial LGG grade 2 (WHO 2016 Classification)<sup>1</sup>; *IDH1* or *IDH2* mutation as determined by direct sequencing or immunohistochemistry (*IDH1* R132H); frozen samples available; TMZ only as a first-line treatment after biopsy or surgical resection(s) introduced between July 2007 and April 2019; ECOG performance status  $\leq 2$  at TMZ initiation; brain MRI in *Digital Imaging and Communications in Medicine* (DICOM) format available at TMZ initiation (baseline) and during follow-up; at least 24 months of follow-up. Patients were excluded if TMZ treatment was administered at another hospital, if TMZ was introduced after the patient experienced an anaplastic transformation of the tumor, or if TMZ treatment was shorter than 6 cycles for reasons other than tumor progression (toxicity or therapeutic choice of the patient and/or oncologist).

All patients were treated with TMZ, days 1–5, every 28 days, 150 mg/m<sup>2</sup>/day for the first cycle and 200 mg/m<sup>2</sup>/day for the subsequent cycles. Treatment initiation was based on radiological criteria (large postsurgical FLAIR tumor residue or tumor FLAIR volume progression). Patients were followed clinically and with MRI every 3–6 months during and following TMZ treatment.

Patients’ data were collected until March 4, 2022. All patients provided consent for translational research. The study was approved by the local Institutional Review Board (authorization #ICM-CORT-2019-2) and the ethics committee of the canton de Vaud (protocol CER-VD 2020-02519) Lausanne, Switzerland.

### Independent Radiological Review and Definition of PFS

The brain MRIs in DICOM format were collected for each patient, from TMZ initiation (baseline MRI) to first progression on or after TMZ-only therapy. Progression was defined according to RANO criteria<sup>20</sup> by 4 independent expert neuro-radiologists (J.M., M.C., A.C., N.M.C.), using the Myrian software (version 2.4.3, Intrasure). Radiologists were blinded to the date of progression according to the clinician in charge of the patient, or the date of the next oncological treatment. Data from this radiological review were interpreted together with clinical data (clinical status of the patient and dose of corticosteroids) to determine the date of progression according to RANO criteria. A duplicate analysis of the longitudinal MRIs of 20 randomly selected patients was performed, stratified for 1p/19q codeletion status and year of initial surgery, by an

independent expert team (T.S. and T.M.) using Myrian software to confirm reproducibility. In addition to the date for PFS-RANO, the date of the next oncological treatment was used to define the next treatment-free survival (NxtTrtFS) as the date of progression as real-world data. Accordingly, PFS-RANO was defined as the interval between initial diagnosis, or the initiation of TMZ treatment (day 1 of first cycle) and the date of progression by RANO criteria or death. The NxtTrtFS was defined as the interval between initial diagnosis, or the initiation of TMZ treatment (day 1 of first cycle) and the next treatment (day 1).

### Ethical Aspects

Patients signed a written informed consent for translational research at the time of surgery. Tumor samples were collected in accordance with institutional guidelines and stored at the Biological Resources Center of the Montpellier University Hospital (BB-0033-00031). Clinical data were extracted from the ICM institutional “Neuro-oncology” database (BDD-NO, CPP Nord-Ouest III, November 4, 2017). The study protocol is in accordance with the French regulation requirements and was approved by the local Institutional Review Board (authorization #ICM-CORT-2019-2, February 18, 2019). The study was approved by the ethics committee of the canton de Vaud, Switzerland (CER-VD, protocol 2020-02519).

### Estimation of the Sample Size

The *MGMTp* methylation score derived from the methylation array is a continuous value obtained through the *MGMT*-STP27 model.<sup>21</sup> The sample size calculation was performed for Cox proportional hazards regression with nonbinary covariates.<sup>22</sup> Based on the TMZ-treated patient cohort ( $n = 57$ ) of the EORTC-22033 study, for which we had 450K methylation data,<sup>19</sup> a set of postulated HRs contained in the range [0.6; 0.9] and 4 different powers (0.7, 0.8, 0.85, and 0.9), associated with  $\alpha = 0.05$ , were evaluated (sizeEpiCont from R package powerSurvEpi). These estimations suggested that a cohort of a hundred patients should reasonably efficiently detect an association between the *MGMTp* methylation score and PFS, defined as the interval from diagnosis to progression or death.

### Biological Material and DNA Methylation Analyses

Tumor specimens (frozen samples) were collected from the Biological Resources Center of the Montpellier University Hospital and reviewed by an expert neuropathologist (V.R.) according to the WHO 2016 classification (*IDH* mutation status; 1p/19q codeletion status). An H&E-stained section was used to mark the compact tumor area ( $\geq 60\%$  of tumor cells). The subsequent serial sections (6  $\times$  100  $\mu$ m, per patient) were transferred into an Eppendorf tube and always kept frozen. DNA and RNA were extracted at the Institute of Pathology of Lausanne University Hospital using the AllPrep DNA/RNA Micro Kit (Qiagen, Cat. No./ID: 80284) on the QIAGEN QIAcube automated system

according to the manufacturer's protocol. The isolated DNA was quantified on Qubit (Thermo Fisher Scientific). The samples were randomized into 2 batches (stratified by time of surgery). The DNA was subjected to bisulfite-conversion with the EZ-96 DNA Methylation-Lightning Kit (Catalog No. D5033, Deep-Well Format) and served as input to high-resolution CpG methylation mapping using the Infinium Methylation EPIC kit (Illumina) and *MGMTp* methylation-specific pyrosequencing. The methylome analyses were performed at the iGE3 Genomics Platform of the University of Geneva, using the protocol for frozen tissues as described by the manufacturer. The dataset is available under the GEO accession number GSE279950 (<http://www.ncbi.nlm.nih.gov/geo/>).

### External Datasets

External datasets comprised the LGG dataset from The Cancer Genome Atlas (TCGA;  $n = 402$ ; 193 WHO grade II, 209 WHO grade III, 1 unspecified WHO grade, dbGaP accession number phs000178.v9.p8; <http://cancergenome.nih.gov>)<sup>23</sup> and a set of anaplastic glioma (NOA-04, WHO grade III,  $n = 227$ ; GEO accession number GSE58218)<sup>24</sup> after quality control and filtering process.

### Preprocessing of DNA Methylation Data

The CpG probes with detection  $P$ -values  $>.01$ , located on the sex chromosomes, or in SNPs were removed. The functional normalization<sup>25</sup> for Illumina 450k and EPIC arrays includes noob (normal-exponential out-of-band) background correction, dye correction (chemistry I vs II), and RUV-2 step (removing unwanted variation) based on control probes. This normalization was performed by the function `preprocessFunnorm` from the R package `minfi`. DNA methylation was summarized by  $M$ -values.<sup>26</sup> The ComBat procedure<sup>27</sup> was used to aggregate the datasets to limit experimental variation and batch effects. The purity of the samples was estimated from DNA methylation data using the R package `InfiniumPurify`.<sup>28</sup>

### Prediction of IDH Mutant Patients

The DNA methylation profiles of the 3 datasets (Montpellier, EORTC-22033, and TCGA-LGG) were analyzed by the multiple factorial analysis (MFA)<sup>29</sup> that allows simultaneous analysis of different data arrays, matched by common columns (same variables) based on principal component analysis. The 3 normalized datasets were weighted by their total inertia for the simultaneous heatmap representation as used in MFA. Similarities between the 3 tables were evaluated by RV (vectorial correlation) coefficient (values between 0 and 1) using R package `ade4` for pairwise RV coefficient permutation tests.<sup>30</sup> The IDH mutation status classification proposed by Yang et al.<sup>31</sup> was projected as supplementary annotation in a heatmap and the representation of patients was projected on the vectorial plan defined by the MFA. Only patients predicted IDH mutants were conserved in this study.

### Copy Number and 1p/19q Codeletion Status

The gene copy number information was assessed using the combined intensities for methylated and unmethylated signals and circular binary segmentation to detect copy number aberration (CNA) events as previously described.<sup>19</sup> The codeletion status of 1p and 19q regions was estimated by classification using a gaussian mixture model.<sup>32</sup> The copy number of marker genes (CNA) was averaged for the chromosomal arm 1p and 19q individually and the 2 new synthetic metrics were used to classify the patients. To increase the accuracy of the procedure, the model was built with multiple datasets (including TCGA-LGG and NOA-04 data) aggregated by the ComBat procedure.<sup>27</sup>

### MGMT-STP27 Model With Extended/Restricted Cutoff

The DNA methylation status of the *MGMTp* and the *MGMT* score (logit-transformed probability) were determined based on HM-450K data as previously reported<sup>18,21</sup> and calculated from EPIC data using the same methylation probes, *cg12434587* and *cg12981137*. The  $M$ -values served as input into the logistic regression model (MGMT-STP27). The cutoff of 0.358 was used for classification into *MGMTp* methylated and unmethylated status, respectively.<sup>18,21</sup> The calculation of the confidence intervals (CIs) for the logistic regression model was performed as described.<sup>18,33</sup> The original binary classification (unmethylated U or methylated M) was *extended* by considering the CI crossing the cutoff. The new groups of *MGMTp* methylation were defined as follows: highly methylated (M); slightly methylated, CI crossing the cutoff (m); mostly unmethylated, CI crossing the cutoff (u), and truly unmethylated (U). CI and *MGMT* classifications can directly be obtained by the function `MGMTpredict` from the R package `mgmtstp27` (version 0.8, <https://github.com/badozor/mgmtstp27>).

### Pyrosequencing for Assessing *MGMTp* Methylation

Determination of *MGMTp* methylation by pyrosequencing using bisulfite-converted DNA was performed according to the protocol and the cutoffs described by Quillien et al.,<sup>34</sup> with minor changes. In brief, the region of interest was amplified by PCR (ZymoTaq DNA Polymerase, Zymo) and subjected to pyrosequencing (PyroMark Q24 Advanced, Qiagen) performed at the Institute of Pathology, CHUV. The average methylation [%] of 5 CpGs (CpGs 74–78; based on CpGs numbered 1–98, genome build GRCh37/hg19, reference, NM\_002412.5) served as input for the calculation of the PYRO *MGMTp* methylation score (logit transformation of the average methylation).

### Statistical Analysis

For the continuous variables, Wilcoxon test ( $t$ ) or Kruskal and Wallis test ( $a$ ) were used to test the differences between 2 or more groups. The independence between qualitative variables and groups was tested with Pearson's chi-squared with Yates' continuity correction or based on the permutation test.

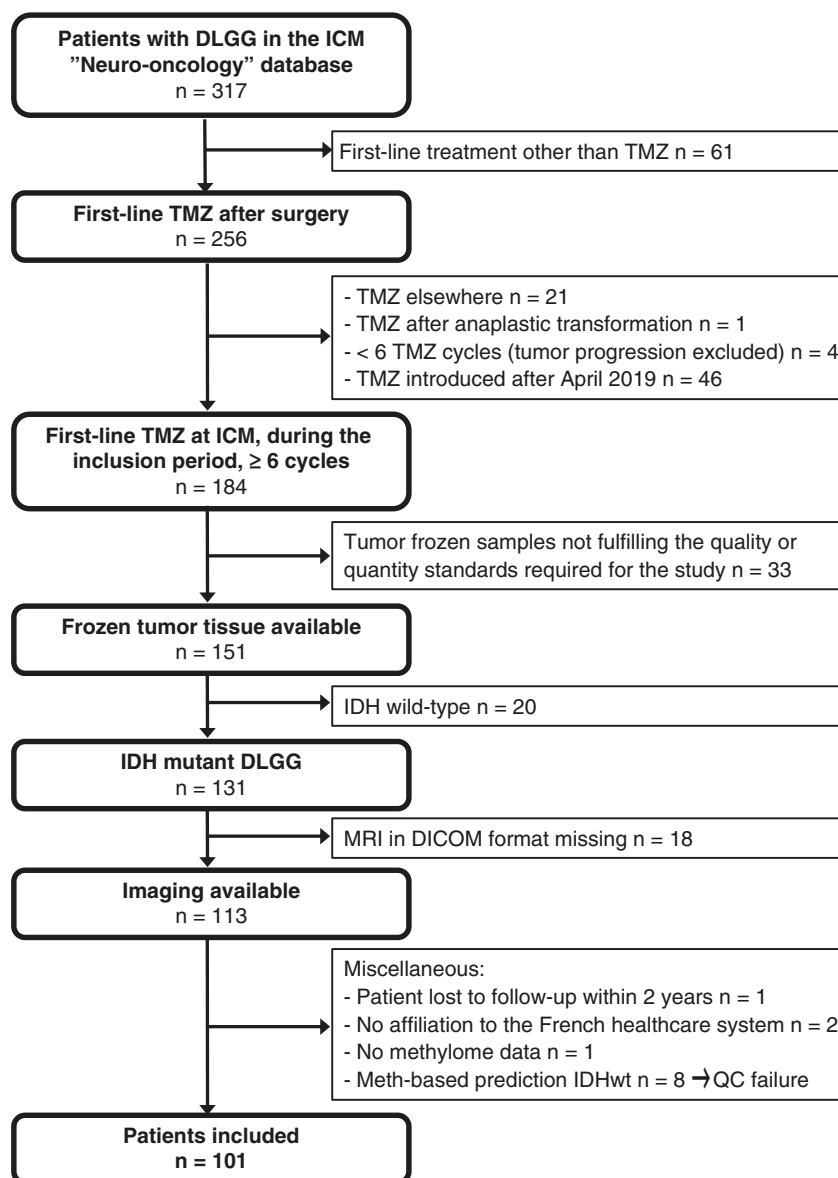


**Figure 1.** Consort diagram of patient selection for the Montpellier test cohort.

The CIs for proportion are given by exact binomial procedure (confidence level = 0.95). Survival univariate and multivariate models were computed by Cox proportional hazards regression model.<sup>35</sup> Analyses and graphical representations were performed using **R-4.4.0** and the R package *rms* and *survival*.

## Results

### Baseline Characteristics of the Test Population (Montpellier)

Based on the eligibility criteria and the availability of methylome data, a total of 101 patients with IDHmt/CIMP

LGG, grade 2 (WHO 2021), who received TMZ only as first-line treatment after surgery(ies), were retained and included in the study (Figure 1, Table 1, Supplementary Figure 1). A sample size of a hundred patients for the test cohort was estimated to be sufficient based on our previous findings in the training cohort.<sup>19</sup> The median age at diagnosis was 35.8 years (range: 18.2–70.1) and 56% of patients were men (Table 1). Tumors were located in the left hemisphere in 54% of patients.

At the time of TMZ initiation, the median age was 39 years (range 21.3–70.3) and 96% of patients had an ECOG performance status of 0–1. The median time interval from tumor diagnosis (first surgery) to TMZ initiation was 35.8 months (range 0.8–191.4) and 24 months (range 0.8–105.6) since the last surgery. One-third (32/101) of the patients had more than 1 surgical intervention prior to TMZ initiation. The surgery

**Table 1.** Baseline Characteristics of the Training and Test Cohorts (EORTC-22033 RT-arm, TMZ-arm; Montpellier, TMZ)

Variable	Modality	N (all)	<sup>1,2</sup> EORTC-RT	<sup>1,2</sup> EORTC-TMZ	<sup>3</sup> Montpellier	<sup>4</sup> P-value (RT and TMZ)	<sup>4</sup> P-value (TMZ-only)
N		63	57	101			
Age at diagnosis—median		221	42 (33, 49)	42 (34, 51)	36 (30, 41)	.001	<b>.003</b>
Age at diagnosis—by class		221				.14	<b>.14</b>
	<=40	24 (38%)	23 (40%)	53 (52%)			
	>40	39 (62%)	34 (60%)	48 (48%)			
Age at TMZ initiation		221	42 (36, 50)	43 (37, 52)	39 (32, 46)	.051	<b>.030</b>
Biological Sex		221				.5	<b>.7</b>
	F	32 (51%)	23 (40%)	44 (44%)			
	M	31 (49%)	34 (60%)	57 (56%)			
<b>Extent of resection</b>							
Surgery at diagnosis		221				–	–
	Biopsy	9 (14%)	4 (7.0%)	10 (9.9%)			
	Partial resection	39 (62%)	40 (70%)	–			
	Total resection	15 (24%)	13 (23%)	–			
	Extent of resection unknown <sup>5</sup>	–	–	91 (90%)			
Surgery preceding TMZ						–	–
	Biopsy	–	–	3 (3.0%)			
	Partial resection	–	–	15 (15%)			
	Subtotal resection	–	–	79 (79%)			
	Total resection	–	–	3 (3.0%)			
	Extent of resection unknown	–	–	1			
WHO performance status at TMZ initiation		221				.3	<b>.2</b>
	0	33 (52%)	32 (56%)	42 (42%)			
	1	26 (41%)	24 (42%)	55 (54%)			
	2	4 (6.3%)	1 (1.8%)	4 (4.0%)			
<sup>†</sup> Time from diagnosis to TMZ [months], median		221	4 (2, 20)	11 (3, 41)	36 (18, 63)	<.001	<b>&lt;.001</b>
<sup>**</sup> Predicted IDH mutant		221					
	Mutant	63 (100%)	57 (100%)	101 (100%)			
1p/19q codeletion (mixture model)		221				.4	<b>.2</b>
	codel	23 (37%)	25 (44%)	34 (34%)			
	non-codel	40 (63%)	32 (56%)	67 (66%)			

**Abbreviations:** IQR, interquartile range; RT, radiotherapy; TMZ, temozolomide.

<sup>†</sup>N (%); Median (IQR).

<sup>‡</sup>Pearson's chi-squared test; Kruskal–Wallis rank sum test; Fisher's exact test.

<sup>§</sup>Tests for all patients only (comparison EORTC-RT, EORTC-TMZ vs Montpellier).

<sup>§</sup>Tests for TMZ-treated patients only (comparison EORTC-TMZ vs Montpellier).

<sup>||</sup>Extent of resection, provided for surgery at diagnosis for EORTC-22033, and for surgery preceding TMZ for the Montpellier cohort.

<sup>†</sup>Time of diagnosis = first surgery.

<sup>\*\*</sup>Prediction based on Yang et al.<sup>31</sup>.

preceding the introduction of TMZ was performed in awake conditions in almost all patients (90.8%) and consisted of total or subtotal resection in 82% of patients. Sixty percent of patients were diagnosed with an astrocytoma, IDHmt,

and 34% with an oligodendroglioma (IDHmt and 1p/19q codeleted). Patients received a median number of 15 cycles of TMZ (range 3–30; 150–200 mg/m<sup>2</sup>/d 5 days of a 28-day cycle). The median number of MRIs per patient was 9 (range 2–23).

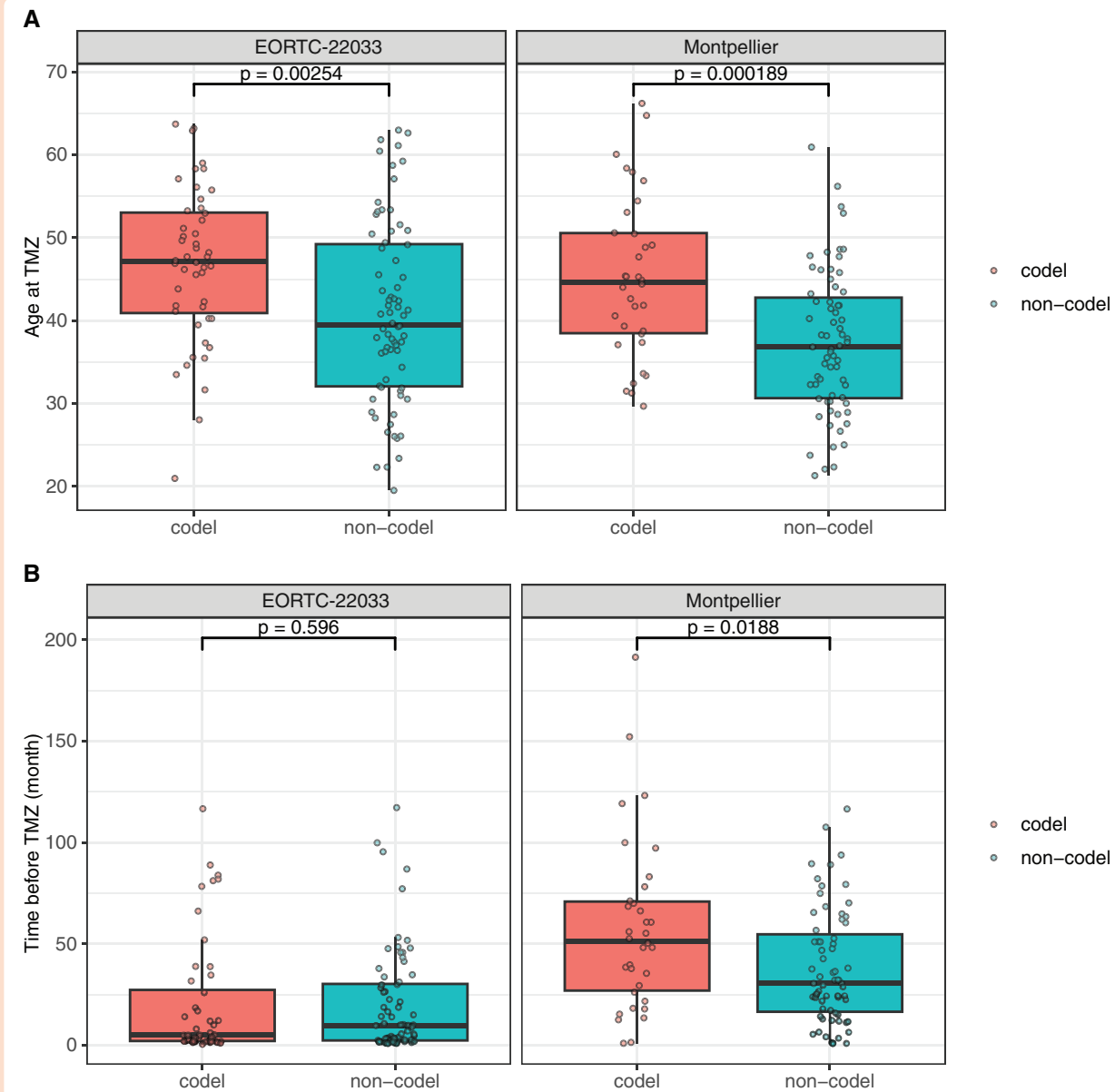


**Figure 2.** Time to temozolamide (TMZ) treatment and patient age, stratified by the 1p/19q codeletion status. The distribution of the patient age (A) and the time interval before initiation of TMZ treatment (B) is shown in box plots for the EORTC-22033—TMZ and the Montpellier cohorts. The figure is split by the 1p/19q codeletion status. The median age of the patients was different between codel and non-codel patients in both cohorts, with higher median age of patients with codel IDHmt LGG (A). The time interval from initial surgery to TMZ treatment initiation in codel versus non-codel patients was different in the Montpellier cohort, but not the EORTC-22033—TMZ cohort (B).

### Comparison of Training and Test Cohorts

The comparison of the baseline characteristics of the patients in the training cohort (EORTC-22033) and the test cohort (Montpellier) is presented in Table 1. The patients enrolled in the EORTC-22033 trial comprised high-risk LGG patients randomized into 2 treatment arms TMZ versus RT at the time when additional treatment beyond surgery was needed, based on defined clinical risk factors.<sup>12</sup> Similarly, the patients in the Montpellier cohort were included if TMZ only was administered as first-line therapy (preferred treatment option of the center, 81%) after surgery(ies) (Figure

1). No differences were observed in the relative ratio of patients with 1p/19q codeleted IDHmt and non-codeleted IDHmt LGG ( $P = .2$ ), biological sex, or the patient performance score at the time of TMZ treatment. A small difference was noted for age at TMZ treatment initiation ( $P = .03$ ), with older patients in the EORTC-22033 training cohort. Expectedly, a marked difference was observed between the cohorts in the median duration of the “watch and wait” time interval between diagnosis and initiation of TMZ treatment (11 [3, 41] vs 36 [18, 63] months,  $P < .001$ ) (Table 1, Figure 2). There was no difference in the median “watch and wait” period between codeleted and non-codeleted

patients in the EORTC-22033 cohort ( $P = .6$ ), while this was significantly different in the Montpellier cohort ( $P = .019$ ), with a longer time interval for the patients with codeleted tumors (Figure 2). Of note, in both cohorts, the “watch and wait” period was highly variable between patients, as illustrated in Supplementary Figure 2. This high variability within and between the 2 cohorts led us to use the time interval from diagnosis/initial surgery to progression after TMZ treatment as PFS for the subsequent survival analyses. The differences between the 2 cohorts likely reflect the distinct inclusion criteria. Of note, the TMZ treatment dose and schedule for the Montpellier IDHmt LGG cohort was different from the high-dose regimen in the EORTC-22033 trial, resulting in an estimated lower cumulative dose of TMZ of 62% of the dose in the EORTC-22033 trial. We hypothesized that *MGMTp* methylation should remain a prominent predictive factor whatever the TMZ schedule used, given the underlying molecular mechanism.

### Evaluation of Progression-Free Survival in the Test Cohort

PFS in the test cohort was determined using RANO criteria after re-review of the longitudinal MRIs. Re-evaluation of 20 randomly selected cases by 2 independent experts revealed a high correlation between these independent reviews of PFS based on RANO criteria (Spearman coefficient  $\rho = 0.97$ ;  $P < .001$ ) and showed no difference in outcome as evaluated by K.M. (Supplementary Figure 3). In addition to PFS with RANO criteria, we report on NxtTrtFS for the Montpellier cohort as real-world data.

For the EORTC-22033 cohort, the PFS data reported in the trial were used. Evaluation of progression was based on investigators' judgment according to the criteria detailed in the protocol for clinical and radiological progression.<sup>12</sup> PFS information for the cohorts is summarized in Supplementary Table 1. Of note, since the baseline characteristics, timing of TMZ introduction and definitions of PFS are not identical between the training and the test cohorts, we abstained from direct comparison.

### *MGMTp* Methylation Score and Association With PFS

To evaluate the pertinence of high *MGMTp* methylation as biomarker for benefit from TMZ in IDHmt LGG patients, we determined the MGMT-STP27-based *MGMTp* methylation score in the 2 cohorts. The methylome of the 2 cohorts is illustrated in a heatmap, annotated for the *MGMTp* methylation scores (Figure 3). For the IDHmt patients, an association of PFS was observed with the *MGMTp* methylation score in the EORTC-22033 cohort treated in the TMZ-arm ( $P = .012$ ), while the codeletion status had no significant effect ( $P = .48$ ) (Figure 4A). In line with the hypothesized predictive effect of *MGMTp* methylation, no significant effect of the *MGMTp* methylation score was observed in the RT-arm, as reported previously<sup>19</sup> (Figure 4B). In the Montpellier cohort, the *MGMTp* methylation score was significantly associated with the NxtTrtFS ( $P = .045$ ), with a significant effect on the codeletion status ( $P = .009$ ), Figure 4C. When considering PFS according to RANO criteria, the

*MGMTp* methylation score almost reached significance ( $P = .07$ ), again with a significant effect of the codeletion status ( $P = .006$ ), Figure 4D.

The association between the MGMT-STP27 score and NxtTrtFS was confirmed using a pyrosequencing-based *MGMTp* methylation score (MGMT-PYROscore) obtained for the same samples ( $P = .002$ , Supplementary Figure 4A). The MGMT-PYROscore was also significantly associated with PFS-RANO ( $P = .004$ , Supplementary Figure 4B). A good correlation was observed between the scores of the 2 assays (Spearman, 0.61;  $P < .001$ ; Supplementary Figure 4C). Pyrosequencing data were only available for the Montpellier cohort.

Of note, a significant difference in the *MGMTp* methylation scores was observed between codeleted and non-codeleted tumors, with higher scores for codeleted tumors (Supplementary Figure 5A), in line with our previous report.<sup>19</sup> This may suggest a confounding effect.

Sample purity may bias the calculation of the *MGMTp* methylation scores. However, no differences in purity were observed between codeleted and non-codeleted tumors of the EORTC-22033 and the Montpellier cohorts ( $P = .754$  and  $P = .980$ , Wilcoxon rank test, Supplementary Figure 5B).

Furthermore, the functionality of *MGMTp* methylation to silence *MGMT* gene expression in both, codeleted and non-codeleted IDHmt LGG, is supported by the strong negative correlation observed between the *MGMTp* methylation score and *MGMT* RNA expression level (Supplementary Figure 6).

### Extension of the MGMT-STP27 Classification

Next, we aimed at defining an *MGMTp* methylation cutoff to establish a biomarker for treatment decisions. However, given the continuous nature of the methylation measures in IDHmt/CIMP LGG, as reported previously,<sup>18,19</sup> no natural cutoff was obvious. Therefore, we used the following strategy, defining “high” *MGMTp* methylation, by extension of the MGMT-STP27 model, for values above the original cutoff and not overlapping with the CI. This was compared to all other samples (other). A significant effect of high *MGMTp* methylation ( $P$ -value = .029, multivariable model) was observed when including all TMZ-treated patients of the training set (EORTC-22033), while the effect of the codeletion status was not significant ( $P = .2$ ) (Figure 5A). A significant effect was also observed for the univariate model ( $P$ -value = .037) including only non-codeleted patients (Supplementary Figure 7B). In contrast, the *MGMTp* methylation status “high” showed no association with PFS in the patients randomized to the RT-arm ( $P = .6$ ), in line with the hypothesized predictive effect for benefit from TMZ (Figure 5B).

Testing the extended MGMT-STP27 classification in the Montpellier cohort revealed no significant association with PFS-RANO or the NxtTrtFS ( $P = .345$ ,  $P = .397$ ; Figure 5C, D). However, the codeletion status was an important factor associated with PFS ( $P < .001$ ,  $P = .011$ ).

The survival results of the multivariable models need to be considered with caution. Indeed, the nonindependence between the codeletion status and the extended



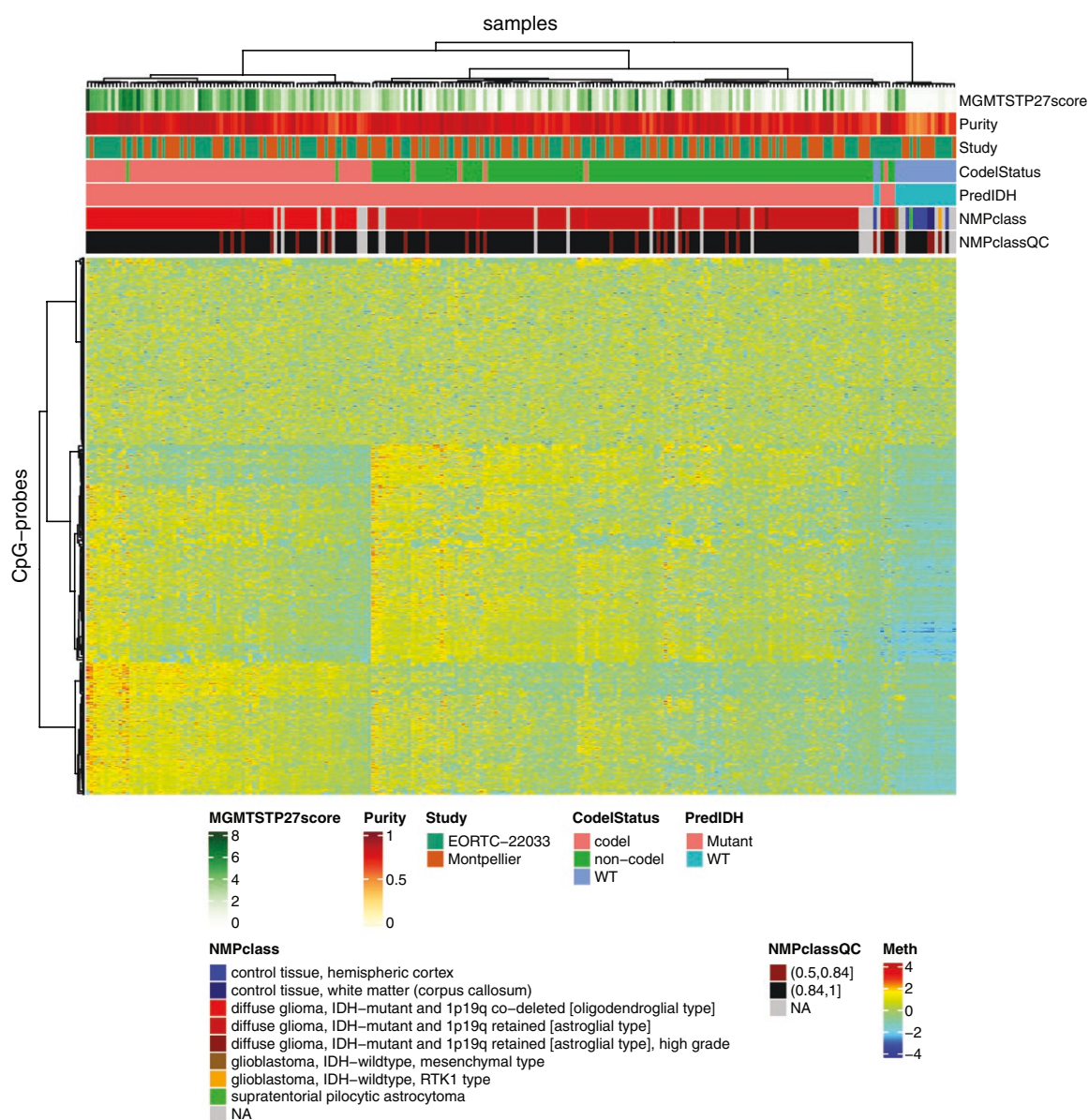


**Figure 3.** The methylome of the low-grade gliomas (LGG) of the 2 patient cohorts. Representation of the 2 complete datasets (EORTC-22033 and Montpellier) including IDH mutant (Mutant) and IDH wild-type (WT) LGG, classified as defined by the model of Yang et al.<sup>31</sup> The heatmap for DNA methylation is based on the 992 most variable common probes. The DNA methylation normalized datasets were weighted by their total inertia for the simultaneous heatmap representation as used in multiple factor analysis (MFA). The dendrograms are based on Euclidean distance and Ward's classification. Additional annotations comprise the MGMT-STP27score, purity, study (cohort), 1p/19q codeletion status, prediction of IDHmt status, and the DNA methylation-based classifications from NMP class, with the NMP class score (version 12.5; NMPclassQC).<sup>36</sup> NA, classification Not Applicable (NMP-class scores <0.5).

MGMT-STP27 classification of *MGMTp* methylation was significant ( $P = .0004$ , Montpellier;  $P = .0368$ , EORTC-22033, Fisher test) (Supplementary Table 2). The highly unbalanced subgroups with small numbers in the no/low methylation groups (1 for EORTC-22033 dataset and 1 for Montpellier dataset) of the codeleted patients precluded proper statistical evaluation of the individual effects of these 2 biomarkers on the outcome. Furthermore, no "high" *MGMTp* methylation effect was observed in the univariate model including only the non-codeleted

patients of the test cohort ( $P = .633$  NxtTrtTFS, and  $P = .627$  PFS-RANO) (Supplementary Figures 7F, H).

Subgroup analyses for the MGMT-STP27 score and the extended MGMT-STP27 classification were performed separately in non-codeleted and codeleted IDHmt LGG (Supplementary Figures 7 and 8). A significant association between the MGMT-STP27 score and PFS was observed for the non-codeleted EORTC-22033 cohort treated by TMZ ( $P = .026$ , Supplementary Figure 7A) and for the codeleted Montpellier cohort ( $P = .029$  NxtTrtTFS, Supplementary Figure 8C).

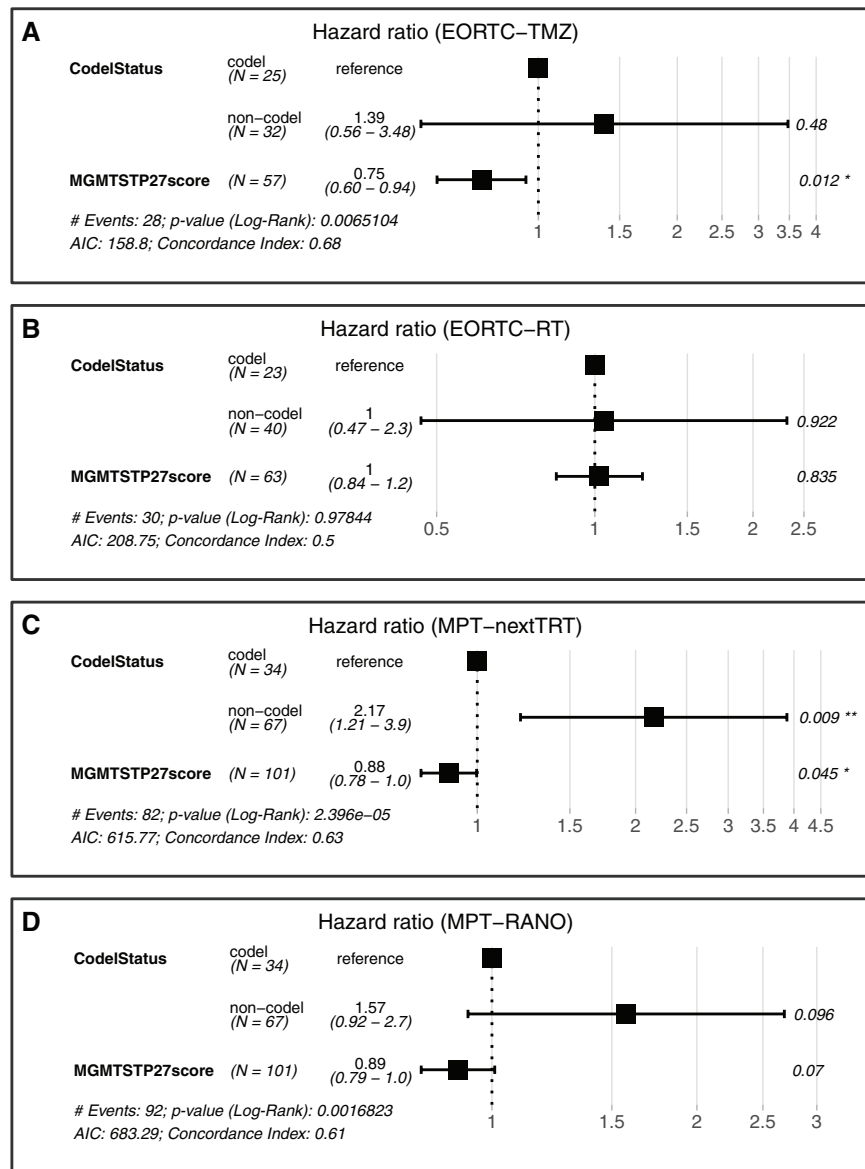


**Figure 4.** Association between progression-free survival (PFS) and the *MGMTp* methylation score. The association of the *MGMTp* methylation score, based on the MGMT-STP27 procedure, with progression-free survival (PFS; interval from diagnosis) was evaluated by the hazard ratio (confidence interval at 95%) from the cox regression model. The forest plots in A and B correspond to the PFS reported for patients treated in EORTC-22033 with temozolomide (TMZ) or radiotherapy (RT), respectively.<sup>12,19</sup> The MGMT-STP27 score was significant in the TMZ treated patients, but not in the patients with RT. The forest plots in C and D visualize the outcome of the Montpellier patients treated with TMZ, with time to progression defined by the next treatment-free survival (NxtTrtFS), and PFS defined by RANO, respectively. The MGMT-STP27 score was significant in the Montpellier cohort when using NxtTrtFS as outcome measure, a trend was observed when using RANO criteria for PFS. \* $P < .05$ ; \*\* $P < .01$ .

## Discussion

The aim of the present project was to improve accurate diagnosis to identify patients with IDHmt LGG who may benefit from TMZ therapy, in order to guide treatment decisions for safe de-escalation of treatment, by delaying radiotherapy. This would allow deferring potential loss of cognitive function, while not compromising oncological

outcome, and thereby improve the QoL of these generally young patients with long survival.

Based on a previous study on a clinical trial cohort for high-risk IDHmt low-grade glioma, we found that the *MGMTp* methylation score (continuous value) and patients with an *MGMTp* methylation “high” status (dichotomized) predicted good outcome in TMZ-treated patients, but not in the RT-treated patients, and independently of the 1p/19q codeletion status. To validate this finding and define a

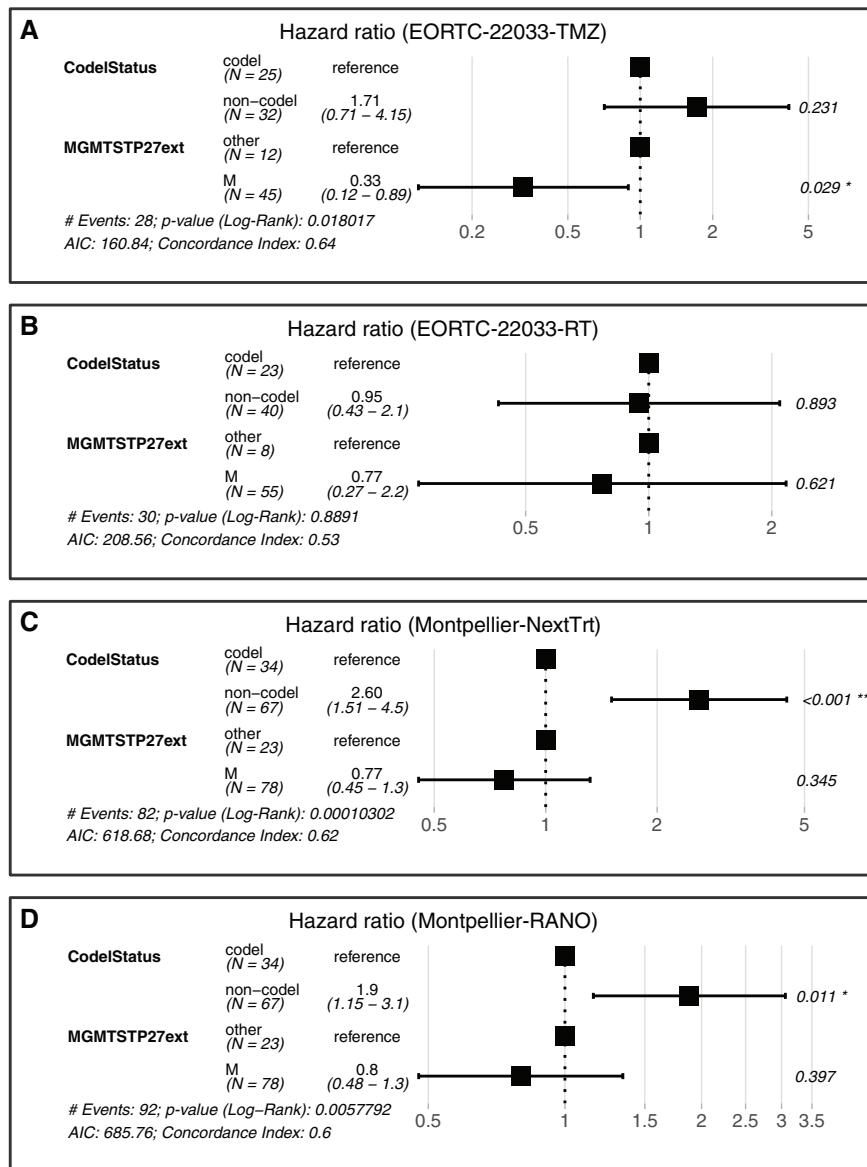


**Figure 5.** Forest plot representation of the association between progression-free survival (PFS) and the extended MGMT-STP27 classification. The association was evaluated by the hazard ratio (confidence interval at 95%) from the cox regression model. The forest plots in A and B correspond to the EORTC-22033 patients treated by temozolomide (TMZ) or radiotherapy (RT), respectively. A significant effect was observed using the extended MGMT-STP27 classification for the TMZ treated patients, but not the patients in the RT-arm. The codel status showed no significant effect. For the Montpellier cohort treated with TMZ, the next treatment-free survival (NxtTrtFS) and the RANO-based PFS estimations, respectively, C and D, no significant effect was observed using the extended MGMT-STP27 classification. However, the codel status was significant. \* $P < .05$ ; \*\*\* $P < .001$ .

cutoff for clinical decision-making, we constituted a validation cohort with patients who received TMZ-only treatment as first-line therapy after surgery/surgeries.

As a main result of this study, we found that the *MGMTp* methylation score was significantly associated with PFS in the EORTC-22033 cohort, and NxtTrtFS in the test cohort, while only a trend was observed using RANO criteria the latter. The definition of PFS in the EORTC-22033 trial may be closer to NxtTrtFS, as no independent review of radiology was performed. The real-world measure of NxtTrtFS may better reflect daily practice. Testing the *MGMTp* methylation score in the real-world validation

cohort in this study confirmed the predicted better outcome in TMZ-treated patients.

However, when testing the effect of the “high” *MGMTp* methylation status on PFS, no significant effect was observed, while the codeletion status was significant in contrast to the clinical trial cohort. The analysis revealed that the 1p/19q codeletion status was the driving factor. Interestingly, less than 5% of 1p/19q codeleted tumors fell below the threshold of “high” methylation classification (1 for EORTC-TMZ dataset and 1 for Montpellier dataset).

The striking difference in the results between the patient cohorts was to its extent unexpected. Some hints, however,

may be explained by the baseline characteristics of the 2 cohorts. The clinical trial cohort enrolled only “high-risk” LGG (WHO grade II) patients, while the real-world data collected in the single-center cohort of the validation set included all LGG patients (WHO grade II) who received TMZ only as first-line chemotherapy (preferred treatment of the center, >80%). Surprisingly, the proportion of 1p/19q codeleted patients was not different between the cohorts ( $P = .11$ ). Similarly, the WHO performance score at the start of TMZ treatment showed no difference ( $P = .3$ ). However, in the time from initial diagnosis to the time when the patients were considered in need of additional treatment and received TMZ, a stark difference was observed, with a median time interval of 11 months (range 3–41) in the training cohort versus 36 months (18–41) ( $P < .001$ ) in the test cohort. The patients in the trial cohort were slightly older at TMZ initiation (43 [37–52] vs 39 [32–46] [ $P = .037$ ]). Furthermore, the total dose of TMZ given in the real world (the test cohort), estimated over 12 cycles in the respective populations, amounted to only 62% of the dose given in the clinical trial cohort and followed a different schedule (5 days week out of 28-day cycle vs 3 weeks out of 4 in the trial cohort). This may have had some impact on the MGMT-mediated effect in the test cohort.

While a prognostic effect for the *MGMTp* methylation score was confirmed in the TMZ-treated IDHmt LGG patients of the validation cohort, we could not validate the cutoff based on the extended MGMT-STP27 classification of “high” *MGMTp* methylation. However, this does not refute the role of MGMT in this disease. The reported acquisition of mutations in the mismatch repair pathway and development of a mutator phenotype in TMZ-treated IDHmt LGG suggests treatment-related selection pressure in tumors with epigenetically silenced *MGMT*.<sup>37,38</sup> The mechanisms and clinical relevance of these TMZ-induced hypermutations in glioma have been extensively discussed elsewhere.<sup>37,38</sup> Furthermore, a predictive effect of *MGMTp* methylation on the benefit from first-line chemo/TMZ treatment on OS was reported from IDHmt astrocytoma WHO grade 4.<sup>39</sup> A relevant difference between IDHmt low-grade glioma and IDHwt glioblastoma may be the recurrent deletion of 1 copy of Chr 10 in glioblastoma, but not in IDHmt LGG, requiring only methylation of 1 *MGMT* allele to shut down MGMT-mediated DNA repair. Furthermore, the driving molecular mechanisms for *MGMTp* methylation are likely different. In IDHmt LGG, it seems to be part of G-CIMP, with higher *MGMTp* methylation scores in codeleted versus non-codeleted IDHmt LGG.

The MGMT-STP27-based assay was bridged to a pyrosequencing-based MGMT assay<sup>34</sup> using the validation cohort samples for which we have obtained both types of data. The methylation scores of the 2 assays showed a good correlation and were both associated with PFS in the test cohort.

Limitations of the study are the retrospective nature and the observed differences in the baseline characteristics, including patient selection criteria, risk factors triggering initiation of TMZ treatment (eg, age > 40 years in the trial), dose and schedule of TMZ treatment, and the definition of the extent of resection prior to TMZ treatment, and clinical trial versus real-world cohort. Nevertheless, the results incite new hypotheses regarding clinical and molecular

parameters relevant to patient management. However, datasets of molecularly characterized IDHmt LGG patients treated uniformly with TMZ only in first line are rare.

Taken together, the analysis of real-world data constituted from a cohort of IDHmt LGG (WHO grade II) patients treated first line with TMZ, did not confirm a prognostic value for the *MGMTp* methylation status after stratification with the 1p/19q codeletion status. Hence, we were not able to confirm that a high *MGMTp* methylation status is a prognostic marker for PFS in TMZ-treated IDHmt LGG patients. However, the 2 patient populations showed significant differences in the watch-and-wait period until additional treatment was required, with a median of less than 1 year (11 months) in the high-risk cohort, enrolled in the EORTC trial, versus almost 3 years (36 months) in the real-world patient cohort. Also, we cannot exclude that the lower dose and different treatment schedules of TMZ impacted the association with *MGMTp* methylation. Interestingly, the proportion between codeleted and non-codeleted patients was not different. Homozygous deletions of *CDKN2A/B* were quasi-absent in both cohorts (1 for Montpellier, 2 for EORTC-TMZ, and 1 for EORTC-RT) and no CIMP-low samples were identified in either cohort. Hence, known genetic and epigenetic features associated with worse outcomes do not explain the difference in this study (Supplementary Table 1).<sup>40,41</sup> This suggests that for good prognosis patients, other currently unknown, molecular and clinical factors may affect outcome in a clinically significant way and remain to be discovered.

## Supplementary Material

Supplementary material is available online at *Neuro-Oncology Advances* ([https://academic.oup.com/noa](https://academic.oup.com/noa/article/7/1/vdae224/7928331)).

## Keywords

IDH mutant low-grade glioma | *MGMTp* methylation score | risk-adjusted treatment

## Conflict of Interest

A.D. has received honoraria for advisory board participation from the following for-profit companies: Novocure, Servier Pharmaceuticals. M.E.H. reports consulting fees to the institution from Servier Pharmaceuticals. All other authors report no competing conflict of interest.

## Funding

This study was funded by The Brain Tumour Charity (CB\_2019/1\_10398, GN-000682 to M.E.H. and A.D.); the Swiss Cancer Research Foundation (KFS-5555-02-2022 to M.E.H.), and the Swiss National Science Foundation (320030\_215718 to M.E.H.). This research was supported by the NIHR Cambridge

Biomedical Research Centre (NIHR203312 to T.M.). The views expressed are those of the authors and not necessarily those of the NIHR or the Department of Health and Social Care.

## Acknowledgments

We are grateful to Cathy Oliver from the International Brain Tumour Alliance for helping us to get input for the project from patients suffering from brain tumors, and thank Nicolas Menjot-de Champfleur from the Montpellier University Medical Center for his collaboration in the project. Many thanks to the Biobanking Laboratory and the Molecular Biology Laboratory at the Institute of Pathology for nucleic acid extraction and pyrosequencing analyses. This work has benefited from the facilities and expertise of the CRB Collection (NEUROLOGIE) of the University Hospital of Montpellier, France ([www.chu-montpellier.fr](http://www.chu-montpellier.fr)). The results presented here are in part based upon data generated by the TCGA Research Network: <https://www.cancer.gov/tcga>.

## Authorship statement:

Conception and design: M.E.H., A.D. P.B., J.D. Acquisition of data (provision of samples, patient data, review of pathology, molecular testing, review of radiology): A.D., K.L., V.R., E.L.B., J.M., M.C., A.C., T.S., T.M., H.D., M.E.H.). Analysis and interpretation of data (eg, statistical analysis, biostatistics, and computational analysis): M.E.H., P.B., A.D. Manuscript writing: M.E.H., P.B., A.D. Review, and/or revision of the manuscript: all coauthors. Study supervision: M.E.H., A.D.

## Data availability:

The methylome data of the EORTC-22033 cohort are available under the accession number GSE104293 at GEO (<http://www.ncbi.nlm.nih.gov/geo/>). The external datasets used, comprised methylome and RNA sequencing (Level 3) data from the LGG dataset of The Cancer Genome Atlas dbGaP accession number phs000178.v9.p8; <http://cancergenome.nih.gov>). The methylome of anaplastic glioma (NOA-04) is available under GEO accession number GSE58218, and the methylome data and *MGMT* gene expression data from the Montpellier cohort, generated in this study, are available under the GEO accession number GSE279950.

## Affiliations

Department of Medical Oncology, Institut Régional du Cancer de Montpellier, University of Montpellier, Montpellier, France (A.D.); Institute of Functional Genomics IGF, University of Montpellier, CNRS, INSERM, Montpellier, France (A.D., V.R., H.D.); Neuroscience Research Center and Service of Neurosurgery, Lausanne University Hospital and University of Lausanne,

Lausanne, Switzerland (P.B., M.E.H.); Translational Data Science & Biomedical Data Science Center, Lausanne University Hospital and University of Lausanne, Lausanne, Switzerland (P.B.); SIB Swiss Institute of Bioinformatics, Lausanne, Switzerland (P.B.); Department of Neuroradiology, I2FH, Institut d'Imagerie Fonctionnelle Humaine, Montpellier University Medical Center, Montpellier, France (J.D., E.L.B.); Department of Neuroradiology, Gui de Chauliac Hospital, Montpellier University Medical Center, Montpellier, France (J.D., E.L.B., J.M., M.C., A.C.); Department of Laboratory Medicine and Pathology, Institute of Pathology, Lausanne University Hospital and University of Lausanne, Lausanne, Switzerland (K.L.); Department of Neuropathology, Gui de Chauliac Hospital, Montpellier University Medical Center, Montpellier, France (V.R.); Department of Neurosurgery, Cambridge University Hospitals NHS Foundation Trust, Cambridge, UK (T.S.); Department of Radiology, University of Cambridge and Cambridge University Hospitals NHS Foundation Trust, Cambridge, UK (T.M.); Department of Neurosurgery, Gui de Chauliac Hospital, Montpellier University Medical Center, Montpellier, France (H.D.); Departments of Oncology and Clinical Neurosciences, L. Lundin and Family Brain Tumor Research Center, Lausanne University Hospital and University of Lausanne, Lausanne, Switzerland (M.E.H.)

## References

- Louis DN, Perry A, Reifenberger G, et al. The 2016 World Health Organization classification of tumors of the central nervous system: a summary. *Acta Neuropathol*. 2016;131(6):803–820.
- Ng S, Rigau V, Moritz-Gasser S, et al. Long-term autonomy, professional activities, cognition, and overall survival after awake functional-based surgery in patients with IDH-mutant grade 2 gliomas: a retrospective cohort study. *Lancet Reg Health Eur*. 2024;46:101078.
- Buckner JC, Shaw EG, Pugh SL, et al. Radiation plus procarbazine, CCNU, and vincristine in low-grade glioma. *N Engl J Med*. 2016;374(14):1344–1355.
- Hervey-Jumper SL, Zhang Y, Phillips JJ, et al. Interactive effects of molecular, therapeutic, and patient factors on outcome of diffuse low-grade glioma. *J Clin Oncol*. 2023;41(11):2029–2042.
- Jakola AS, Skjulsvik AJ, Myrnes KS, et al. Surgical resection versus watchful waiting in low-grade gliomas. *Ann Oncol*. 2017;28(8):1942–1948.
- Mandonnet E, Duffau H. An attempt to conceptualize the individual onco-functional balance: why a standardized treatment is an illusion for diffuse low-grade glioma patients. *Crit Rev Oncol Hematol*. 2018;122:83–91.
- Ruda R, Soffietti R. Controversies in management of low-grade gliomas in light of new data from clinical trials. *Neuro Oncol*. 2017;19(2):143–144.
- Schiff D, van den Bent M, Vogelbaum MA, et al. Recent developments and future directions in adult lower-grade gliomas: Society for Neuro-Oncology (SNO) and European Association of Neuro-Oncology (EANO) consensus. *Neuro Oncol*. 2019;21(7):837–853.
- Weller M, van den Bent M, Tonn JC, et al.; European Association for Neuro-Oncology (EANO) Task Force on Gliomas. European Association for Neuro-Oncology (EANO) guideline on the diagnosis and treatment of adult astrocytic and oligodendroglial gliomas. *Lancet Oncol*. 2017;18(6):e315–e329.

10. Mellinghoff IK, van den Bent MJ, Blumenthal DT, et al.; INDIGO Trial Investigators. Vorasidenib in IDH1- or IDH2-mutant low-grade glioma. *N Engl J Med.* 2023;389(7):589–601.
11. Schiff D. Headway against brain tumors with molecular targeting of IDH-mutant gliomas. *N Engl J Med.* 2023;389(7):653–654.
12. Baumert BG, Hegi ME, van den Bent MJ, et al. Temozolomide chemotherapy versus radiotherapy in high-risk low-grade glioma (EORTC 22033-26033): a randomised, open-label, phase 3 intergroup study. *Lancet Oncol.* 2016;17(11):1521–1532.
13. Douw L, Klein M, Fagel SS, et al. Cognitive and radiological effects of radiotherapy in patients with low-grade glioma: long-term follow-up. *Lancet Neurol.* 2009;8(9):810–818.
14. van den Bent MJ, Afra D, de Witte O, et al.; EORTC Radiotherapy and Brain Tumor Groups and the UK Medical Research Council. Long-term efficacy of early versus delayed radiotherapy for low-grade astrocytoma and oligodendroglioma in adults: the EORTC 22845 randomised trial. *Lancet.* 2005;366(9490):985–990.
15. Darlix A, Mandonnet E, Freyschlag CF, et al. Chemotherapy and diffuse low-grade gliomas: a survey within the European Low-Grade Glioma Network. *Neurooncol. Pract.* 2019;6(4):264–273.
16. Hegi ME, Diserens AC, Gorlia T, et al. MGMT gene silencing and benefit from temozolomide in glioblastoma. *N Engl J Med.* 2005;352(10):997–1003.
17. Hegi ME, Stupp R. Withholding temozolomide in glioblastoma patients with unmethylated MGMT promoter—still a dilemma? *Neuro Oncol.* 2015;17(11):1425–1427.
18. Bady P, Delorenzi M, Hegi ME. Sensitivity analysis of the MGMT-STP27 model and impact of genetic and epigenetic context to predict the MGMT methylation status in gliomas and other tumors. *J Mol Diagn.* 2016;18(3):350–361.
19. Bady P, Kurscheid S, Delorenzi M, et al. The DNA methylome of DDR genes and benefit from RT or TMZ in IDH mutant low-grade glioma treated in EORTC 22033. *Acta Neuropathol.* 2018;135(4):601–615.
20. Wen PY, Chang SM, Van den Bent MJ, et al. Response assessment in neuro-oncology clinical trials. *J Clin Oncol.* 2017;35(21):2439–2449.
21. Bady P, Sciuscio D, Diserens AC, et al. MGMT methylation analysis of glioblastoma on the Infinium methylation BeadChip identifies two distinct CpG regions associated with gene silencing and outcome, yielding a prediction model for comparisons across datasets, tumor grades, and CIMP-status. *Acta Neuropathol.* 2012;124(4):547–560.
22. Hsieh FY, Lavori PW. Sample-size calculations for the Cox proportional hazards regression model with nonbinary covariates. *Control Clin Trials.* 2000;21(6):552–560.
23. Brat DJ, Verhaak RG, Aldape KD, et al.; Cancer Genome Atlas Research Network. Comprehensive, integrative genomic analysis of diffuse lower-grade gliomas. *N Engl J Med.* 2015;372(26):2481–2498.
24. Wiestler B, Capper D, Sill M, et al. Integrated DNA methylation and copy-number profiling identify three clinically and biologically relevant groups of anaplastic glioma. *Acta Neuropathol.* 2014;128(4):561–571.
25. Fortin JP, Labbe A, Lemire M, et al. Functional normalization of 450k methylation array data improves replication in large cancer studies. *Genome Biol.* 2014;15(12):503.
26. Du P, Zhang X, Huang CC, et al. Comparison of Beta-value and M-value methods for quantifying methylation levels by microarray analysis. *BMC Bioinf.* 2010;11:587.
27. Johnson WE, Li C, Rabinovic A. Adjusting batch effects in microarray expression data using empirical Bayes methods. *Biostatistics.* 2007;8(1):118–127.
28. Qin Y, Feng H, Chen M, Wu H, Zheng X. InfiniumPurify: an R package for estimating and accounting for tumor purity in cancer methylation research. *Genes Dis.* 2018;5(1):43–45.
29. Escoufier B, Pages J. Multiple factor analysis (AFMULT package). *Comput Stat Data Anal.* 1994;18(1):121–140.
30. Heo M, Gabriel KR. A permutation test of association between configurations by means of the rv coefficient. *Commun Stat Simul Comput.* 1998;27(3):843–856.
31. Yang J, Wang Q, Zhang ZY, et al. DNA methylation-based epigenetic signatures predict somatic genomic alterations in gliomas. *Nat Commun.* 2022;13(1):4410.
32. Scrucca L, Fraley C, Murphy TB, Raftery AE. *Model-Based Clustering, Classification and Density Estimation Using Mclust in R.* New York, NY: Chapman & Hall/CRC Press; 2023.
33. Faraway JJ. *Extending Linear Models with R: Generalized Linear, Mixed Effects and Nonparametric Regression Models.* Boca Raton, FL: Chapman & Hall/CRC; 2006.
34. Quillien V, Lavenu A, Ducray F, et al. Validation of the high-performance of pyrosequencing for clinical MGMT testing on a cohort of glioblastoma patients from a prospective dedicated multicentric trial. *Oncotarget.* 2016;7(38):61916–61929.
35. Therneau TM, Grambsch PM. *Modeling Survival Data: Extending the Cox Model.* New York: Springer; 2000.
36. Capper D, Jones DTW, Sill M, et al. DNA methylation-based classification of central nervous system tumours. *Nature.* 2018;555(7697):469–474.
37. Mathur R, Zhang Y, Grimmer MR, et al. MGMT promoter methylation level in newly diagnosed low-grade glioma is a predictor of hypermutation at recurrence. *Neuro Oncol.* 2020;22(11):1580–1590.
38. Touat M, Li YY, Boynton AN, et al. Mechanisms and therapeutic implications of hypermutation in gliomas. *Nature.* 2020;580(7804):517–523.
39. Lim-Fat MJ, Wen PY, Touat M, Puduvalli VK, Iorgulescu JB. MGMT promoter methylation and survival following chemotherapy for WHO grade 4 IDH-mutant astrocytoma. *Neuro Oncol.* 2024;26(12):2388–2390.
40. Malta TM, de Souza CF, Sabedot TS, et al. Glioma CpG Island Methylator Phenotype (G-CIMP): biological and clinical implications. *Neuro Oncol.* 2017;20(10):608–620.
41. Shirahata M, Ono T, Stichel D, et al. Novel, improved grading system(s) for IDH-mutant astrocytic gliomas. *Acta Neuropathol.* 2018;136(1):153–166.